Peer-reviewed version available at *Inorganics* **2018**, *6*, 101; doi:10.3390/inorganics6040101

Communication

Exploring High-Symmetry Lanthanide-Functionalized Polyoxopalladates as Building Blocks for Quantum Computing

José J. Baldoví [1,*], Aleksandar Kondinski [2,*]

[1] Max Planck Institute for the Structure and Dynamics of Matter, Luruper Chaussee 149, DE-22761 Hamburg, Germany;
[2] Department of Chemistry, KU Leuven, Celestijnenlaan 200F, B-3001 Leuven, Belgium;
* Correspondence: jose.baldovi@mpsd.mpg.de Tel.: +49 (0)40-8998-88324, aleksandar.kondinski@kuleuven.be Tel.: +32 16 37 29 41;

Abstract: The structural, electronic and magnetochemical properties of the star-shaped polyoxopalladate $[Pd_{15}O_{10}(SeO_3)_{10}]^{10-}$ (POPd) and its lanthanide functionalized derivatives have been investigated on the basis of density functional theory followed by a ligand field analysis using the Radial Effective Charge (REC) model. Our study predicts that heteroPOPd is a robust cryptand that enforces D_{5h} symmetry around the encapsulated Ln^{3+} centers. This rigid coordination environment favors interesting potential magnetic behavior in the Er and Ho derivatives, which may be of interest for molecular spintronics and quantum computing applications.

Keywords: lanthanides, single-ion magnets, spin qubits, polyoxopalladates, density functional theory.

1. Introduction

Quantum computing is an emerging area of research based on the explicit use of quantum-mechanical phenomena to implement logic operations for the purposes of highly-efficient information and communication technologies. In contrast to conventional computers which store information in one of the two definite states '0' or '1', the basic units of a quantum computer are quantum bits (qubits), which can be a superposition of the basis states. Within this new paradigm, magnetic molecules are quantum two-levels systems that have been proposed as promising candidates to build up quantum computers.[1-6] In this regard, magnetic molecules exhibit remarkable structural and chemical versatility, tunable physicochemical properties and inherent scalability, considering the enormous opportunities of (self-)organization.[7] Although the current prospects for their technological implementation remain elusive due to challenges such as loss of quantum coherence,[8] many recent advances in the field have been encouraging. [9-14]

In this context, polyoxometalate (POM) chemistry has shown some advantageous chemical, structural and electronic features such as robustness, highly-symmetrical encapsulating environments and absence of nuclear spins around the magnetic ion.[15] Indeed, lanthanide-based polyoxometalates (POMs) are among the first examples of single-ion magnets (SIMs)[16] and have also contributed to the field of molecular spin qubits.[17,18] Some relevant examples in molecular magnetism include two families of lanthanide-containing polyoxomolybdates[19] and the cube-shaped polyoxopalladates (POPds).[20]

In this work, we focus on a different series of lanthanide-containing POPds as model systems with the aim to rationally design new molecular nanomagnets. This polynuclear, negatively charged nanocluster is the star-shaped Delferro-Hu $[Pd_{15}Se_{10}O_{40}]^{10-}$ (**1**) polyanion (Figure 1a)[21,22] which exhibits internal cavity defined by ten oxo ligands positioned at the vertices of a virtual pentagonal prism that is suitable for encapsulation of metal cations and water molecules (Figure 1b).[21-25] In comparison to

the other available phosphate or phenyl arsenate capped derivatives,[21-25] its chemical structure exhibits relatively low negative charge and the lowest number of atoms, whereas it retains the high overall D_{5h} symmetry. Using density functional theory (DFT) we initially explore the diamagnetic $[NaPd_{15}Se_{10}O_{40}]^{9-}$ (**1-Na**) POPd system and we find a suitable level of theory that can accurately estimate the geometry of the inner cavity. As a second step, we calculate and discuss the structural and electronic properties of three lanthanide encapsulating model systems with general formula $[LnPd_{15}Se_{10}O_{40}]^{7-}$, where Ln = La(**1-La**), Gd(**1-Gd**) and Lu(**1-Lu**). Finally, we use the optimized molecular geometry of the Gd^{3+} derivative to explore the spin energy levels and ground doublet composition of the Tb^{3+}(**1-Tb**), Dy^{3+}(**1-Dy**), Ho^{3+}(**1-Ho**) and Er^{3+}(**1-Er**) derivatives. Our approach provides an inexpensive estimation of the potential of these analogues as molecular nanomagnets.

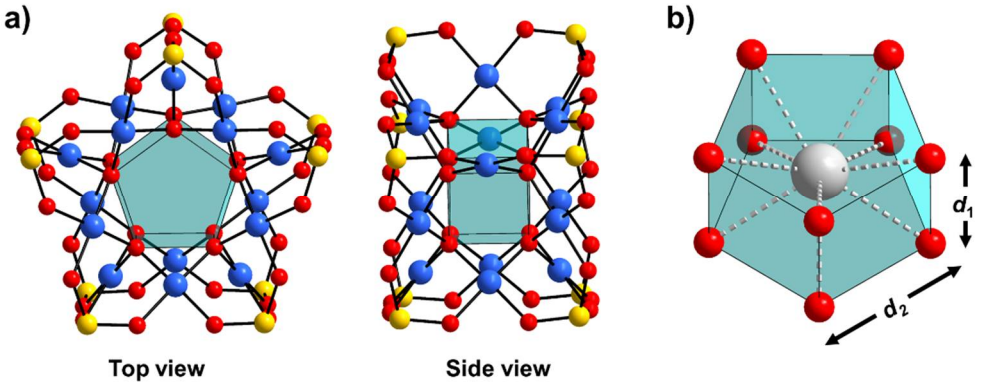

Figure 1. Combined polyhedral and ball-and-stick representation polyanion **1** (a) with detail on the inner cavity suitable for encapsulation of metal cations (b). The assigned d_1 and d_2 refer to interatomic O···O distances that define the size of the inner cavity (*vide infra*). Color code: Se = yellow, Pd = blue and O = red spheres, $\{O_{10}\}/\{MO_{10}\}$ = cyan transparent polyhedra.

2. Results and Discussion

2.1. Structural and electronic properties

The structural and electronic properties of **1, 1-Na, 1-La, 1-Gd and 1-Lu** were investigate by means of relativistic density functional theory (DFT) as implemented in the ADF code.[26] The geometry of **1-Na** in water was followed at different theoretical levels (Table S1) that have been previously successfully used for an accurate estimation of the structure of noble metal-based POMs.[27-30] Considering that for the ligand field analysis it is more essential to have geometries that primarily provide an accurate estimation of positions of the oxo ligands that coordinate to the encapsulated lanthanide centers, we have found that geometry optimization calculations of the model system **1-Na** at BP86/TZ2P/ZSC/COSMO-water level provide the most accurate approximation of the coordination environment around the Na^+ center, while the Pd-O and Se-O bonds are also well approximated (see Table S1). Subsequently, polyanions **1**, **1-La, 1-Gd and 1-Lu** were optimized at this level as well. All insights on the electronic structure and bonding energies are discussed based on single point calculation performed at (U)B3LYP/TZ2P/ZSC/COSMO-water level (see SI).

Our calculations show that polyanions **1, 1-Na, 1-La, 1-Gd and 1-Lu** exhibit very narrow Se-O, Pd-O(Pd), Pd-O(Se) bond lengths in the ranges of 1.731-1.733 Å, 1994-2.008 Å and 2.058-2.092 Å respectively (Table S2). The interatomic distances d_1(O···O) and d_2(O···O) that define the internal pentagonal cavity (Figure 1b) are found on the range of 2.646-2.701 Å and 2574-2672 Å respectively. The changes induced by encapsulation of the different cations are on the range of < 0.1 Å, which implies that the internal cavities are generally unaffected by the encapsulation. The calculated Ln-O bonds/distances are in the range of 2.559-2.644 Å, which are characteristic for lanthanide-containing POM systems.[16-20]

The optimized systems **1-La, 1-Gd and 1-Lu** exhibit a gap energy of ca 3.5-3.6 eV between the highest occupied and the lowest unoccupied molecular orbital (i.e. HOMO and LUMO). The high gap energy is comparable to that of the reported polyanions **1** (3.4 eV) and **1-Na** (3.5 eV), which

substantiates that the proposed lanthanide encapsulating systems exhibit significant intrinsic stability making them promising candidates for future preparation (See Table S4). The HOMO in systems **1-La, 1-Gd and 1-Lu** is doubly degenerate and is composed of Pd-centered d_{xy}- and d_{yz}-type orbitals and O-centered p-type orbitals (Figure 2a). The LUMO in **1-La, 1-Gd and 1-Lu** is also doubly degenerate and populates mainly O and Pd centers but also minorly Se^{4+} and Ln^{3+} centers (Figure 2a). The antibonding LUMO exhibits nodes between the Pd-centered $d_{x^2-y^2}$-type orbitals and O-centered p-type orbitals, suggesting that population of this molecular orbital (*e.g. via* electrochemical reduction) can destabilize these bonds. The transition between the HOMO to LUMO corresponds predominantly to *d-d* transitions accompanied by metal to ligand charge transfer (Pd→ O) (Table S5).

In our view polyanions **3**-**9** can be potentially prepared in two steps approach, where polyanions **1** or **2** serve as precursors and are reacted with the lanthanide trications to yield $[LnPd_{15}Se_{10}O_{40}]^{7-}$, either by direct encapsulation or by Na^+ cation exchange. Some aspects of the DFT calculations substantiate this opportunity. First polyanions **1** and **1-Na** exhibit pentagonal entrance defined by five oxo ligands that is comparable in size to that of the Preyssler type polyoxoanions (Figure S1) which is well-known to permeate lanthanide cations.[16] The inscribed virtual radius of the pentagonal entrance in **1** is ca. 1.79 Å, which is significantly larger than the effective ionic radius of the bare lanthanide trications.[31] Second, Mulliken charge analysis (Table S3) and molecular electrostatic potential (Figure 2b) of **1** show that the inner oxygen atoms defining the inner cavity are highly negatively charged and thus very nucleophilic. The high nucleophilicity of the inner cavity is the driving force for encapsulation of Na^+ showing favorable binding energies of -201.2 kcal/mol, which is in line with the experimental evidence.[21] In contrast the lanthanide trications show few times more negative binding energies which increase along the lanthanide series (La^{3+} = -983.9 kcal/mol, Gd^{3+} = -1031.1 kcal/mol and Lu^{3+} = -1060.6 kcal/mol).

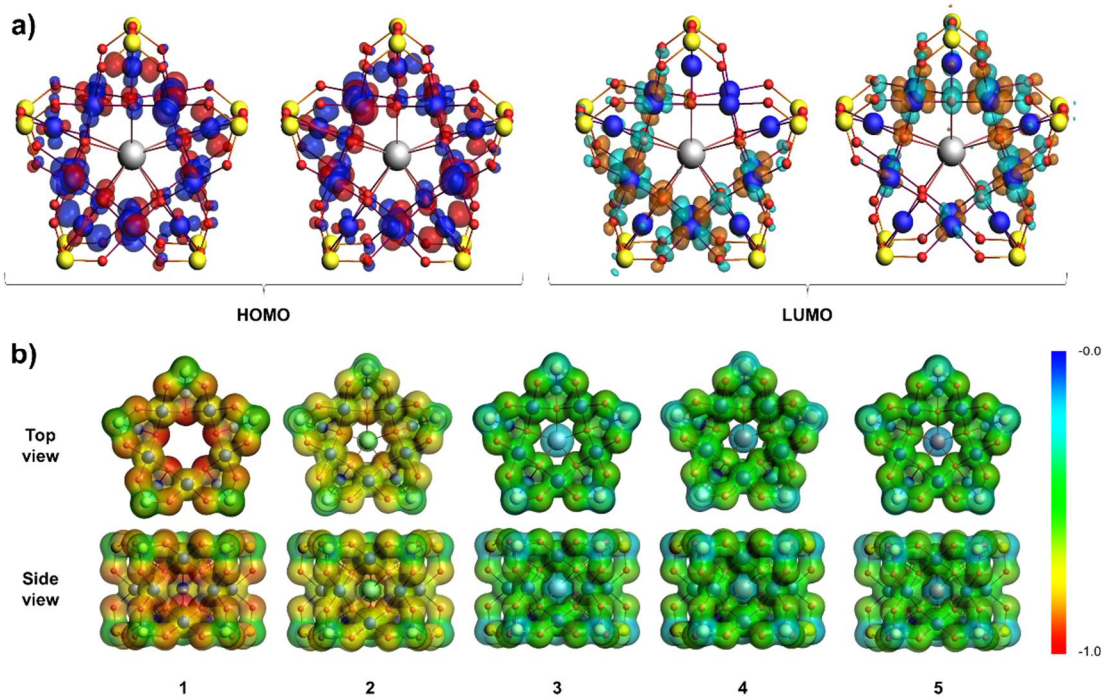

Figure 2. (a) The doubly degenerate HOMO and LUMO of **1-La** which is also representative for **1-Gd** and **1-Lu**; (b) MEP plotted over the density isosurface of polyanions **1-5**. Most negative potentials are colored in red. All calculations are performed at (U)B3LYP/TZ2P/ZSC/COSMO-water level. Color code: Se = yellow, Pd = blue and O = red spheres.

2.2. Ligand field analysis

Starting from the DFT-relaxed structure of the **1-Gd**, we have applied the Radial Effective Charge (REC) model using the SIMPRE computational package to the **1-Tb**, **1-Dy**, **1-Ho** and **1-Er**

derivatives.[32,33] This parametric model introduces covalency effects by placing an effective charge at an effective distance determined by a radial displacement D_r (see Section 5 of SI for details). One of its main advantages is that, for similar families of homoleptic coordination complexes, such parameters are reusable, allowing an inexpensive determination of the spectroscopic and magnetic properties.[34] Thus, we have taken advantage of the *semi-empirical* information of the recently reported $[LnPd_{12}(AsPh)_8O_{32}]^{5-}$ series[20] to provide an estimation of the ligand field splitting of the ground-*J* multiplet as well as the ground state composition of each derivative. As the coordination number in these two families of POPds is different, 8 in the case of $[LnPd_{12}(AsPh)_8O_{32}]^{5-}$ and 10 in $[LnPd_{15}Se_{10}O_{40}]^{7-}$ and we do not have access to the X-ray structures, we have explored different possibilities for the REC parameters, always keeping constant the total $f=D_r \cdot Z_i$ product.[35] The scanning of the REC parameters at different levels of covalency allows us to evaluate the robustness of the composition of the ground state with the aim of identifying which candidates are more suitable to exhibit single-molecule magnet behavior. The resulting energy level pattern as a function of the value of the radial displacement for **1-Tb**, **1-Dy**, **1-Ho** and **1-Er** is reported in Figure 3.

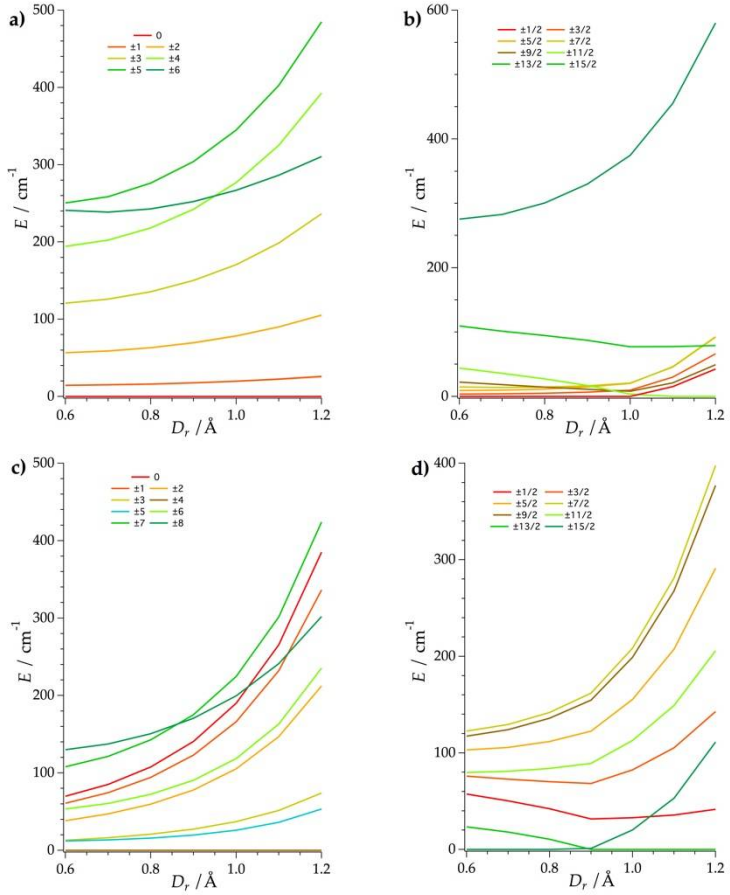

Figure 3. Energy level scheme of the (a) **1-Tb**, (b) **1-Dy**, (c) **1-Ho** and (d) **1-Er** as a function of D_r using the REC model. The different colors indicate the main M_J contribution to the wave function.

A general trend that one can observe in the evolution of the energy levels versus D_r is that the larger the covalent correction, the larger the total ligand field splitting. This is related with the $1/(R_i^{K+1})$ dependence of the k=2,4,6 ligand field parameters in the model, where R_i is the effective distance between the point charge and the Ln^{3+} ion (see Section 5 of SI, equations 2a, 2b and 2c). Due to the almost perfect D_{5h} geometry around the lanthanide, the extradiagonal ligand field B_{kq} parameters, which are responsible of the mixing between M_J microstates, are practically negligible. This results in almost pure wave functions (~100% $|M_J\rangle$) (Table S7). Regarding the ground state compositions, one can notice that for the non-Kramers ions (**1-Tb** and **1-Ho**) the same M_J is the most stable along our

exploration. In the case of **1-Tb**, the equatorial geometry of $\{Pd_{15}Se_{10}O_{40}\}$ yields to a diamagnetic state $M_J = 0$, whereas for **1-Ho** the ground state is composed by two ±4 microstates. This suggests that we can practically discard the **1-Tb** as a molecular nanomagnet, whereas the **1-Ho** derivative is a potential candidate as a two-level quantum system, as long as small distortions in the real structure of the complex create a sufficiently large tunneling splitting between these two states.[17] On the other hand, the ground states of the **1-Dy** and **1-Er** derivatives present two different possibilities based on our magnetostructural investigation. Thus, we cannot state accurately the main M_J contribution to the ground doublet of these systems as it will be very sensitive to the real coordinates of the compounds. However, whereas the **1-Dy** analogue can be either ±1/2 or ±11/2, the **1-Er** analogue is clearly the most promising of the series, as the model consistently predicts a ground state determined by a pure high M_J microstate (either ±15/2 or ±13/2). This preference of the polyoxoanion for stabilizing larger spin microstates in **1-Er** is a direct consequence of the equatorial distribution of the electrostatic charge around the magnetic center[5,36] Thus, according to our calculations, we can conclude that compound **1-Ho** presents an interesting composition of the ground state to design a molecular spin qubit with possible operating points, whereas **1-Er** has a very favorable coordination environment to exhibit slow relaxation of the magnetization.

3. Conclusions

In summary, we have theoretically investigated the structural, electronic and magnetic properties of a high-symmetry molecular structure based on POPds. Our calculations based on density functional theory and a ligand field approach indicate that the rigid coordination environment leads to almost pure spin states in all the systems of the series. The equatorially-expanded charge distribution around the lanthanide favors the stabilization of a high-spin ground doublet in the **1-Er** derivative, which can be considered as a potential single-ion magnet. On the other hand, the ground state of the **1-Ho** derivative offers an interesting playground to break ±4 degeneracy through ligand-field-induced tunneling splitting which can be of interest for quantum computing applications. Our efforts to shed more experimental light on these systems are currently underway.

Supplementary Materials: The following are available online at www.mdpi.com/xxx/s1. Figure S1: Combined ball-and-stick and polyhedral representation of the $[P_5W_{30}O_{110}]^{15-}$ polyanion shown in top (left) and side view (right). Figure S2. Ball-and-stick representation depicting segment of the **1**, **1-Na**, **1-La**, **1-Gd** and **1-Lu** polanions. Figure S3: Spin density isosurface of **1-Gd** indicating accumulation of α spins at the Gd^{III} center as calculated at UB3LYP/TZ2P/ZSC/COSMO level. Color code: Pd = blue, O = red, and Se = yellow spheres. Table S1: Characteristic bond lengths of polyanion **1-Na** system as calculated at different theoretical levels. Table S2 Characteristic bond lengths and interatomic distances in polyanions **1**, **1-Na**, **1-La**, **1-Gd** and **1-Lu** as calculated at BP/TZ2P/ZSC/COSMO-water levels. Table S3: Mulliken charge populations of **1**, **1-Na**, **1-La**, **1-Gd** and **1-Lu** obtained at (U)B3LYP/TZ2P/ZSC/ COSMO for different O atoms following the labeling in Figure S2. Table S4: HOMO, LUMO and HOMO-LUMO gap (ΔLUMO-HOMO) energies in eV of **1**, **1-Na**, **1-La**, **1-Gd** and **1-Lu**, calculated at (U)B3LYP/TZ2P/ZSC/COSMO. Table S5: Contributions (in %) of the Kohn-Sham orbitals centered on palladium, oxygen, selenium and the incorporated cations to the HOMO and the LUMO orbitals of **1**, **1-Na**, **1-La**, **1-Gd** and **1-Lu**. Table S6. Crystal-field parameters ($A_k^q < r^k >$; Stevens notation) in cm^{-1} calculated for **1-Tb**, **1-Dy**, **1-Ho** and **1-Er.** Table S7. Ground multiplet energy level scheme (cm^{-1}) and main |MJ> contributions to the wave function calculated for **1-Tb**, **1-Dy**, **1-Ho** and **1-Er**.

Author Contributions: JJB conceived the original idea on this project. JJB and AK conceptualized the project, generated, analyzed and discussed the results and contributed in writing the manuscript.

Funding: JJB thanks the EU for a Marie Curie Fellowship (H2020-MSCA-IF-2016-751047). AK thanks Research Foundation Flanders (FWO) for postdoctoral research grant (166497/12Y9218N LV 5457).

Acknowledgments: Max Planck Institute for the Structure and Dynamics of Matter (MPSD) and KU Leuven are thanked for research support.

Conflicts of Interest: The authors declare no conflict of interest.

References

1. Hill, S.; Edwards, R. S.; Aliaga-Alcalde, N.; Christou, G. Quantum Coherence in an Exchange-Coupled Dimer of Single-Molecule Magnets. *Science* **2003**, 302(5647), 1015–1018, DOI: 10.1126/science.1090082.
2. Cerletti, V.; Coish, W. A.; Gywat, O.; Loss, D. Recipes for spin-based quantum computing. *Nanotechnology* **2005**, 16(4), R27, DOI: 10.1088/0957-4484/16/4/R01.
3. Bertaina, S.; Gambarelli, S.; Mitra, T.; Tsukerblat, B.; Müller, A.; Barbara, B. Quantum oscillations in a molecular magnet. *Nature* **2008**, 453, 203–206, DOI: 10.1038/nature06962.
4. Stamp, P. C. E.; Gaita-Ariño, A. Spin-based quantum computers made by chemistry: hows and whys. *J. Mater. Chem*. **2009**, 19 (12), 1718–1730, DOI:10.1039/B811778K.
5. Baldoví, J. J.; Cardona-Serra, S.; Clemente-Juan, J. M.; Coronado, E.; Gaita-Ariño, A.; Palii, A. Rational Design of Single-Ion Magnets and Spin Qubits Based on Mononuclear Lanthanoid Complexes. *Inorg. Chem.* **2012**, 51(22), 12565–12574, DOI: 10.1021/ic302068c.
6. Atzori, M.; Morra, E.; Tesi, L.; Albino, A.; Chiesa, M.; Sorace, L.; Sessoli, R. Quantum Coherence Times Enhancement in Vanadium(IV)-based Potential Molecular Qubits: the Key Role of the Vanadyl Moiety. *J. Am. Chem. Soc.* **2016**, 138, 11234–11244, DOI: 10.1021/jacs.6b05574.
7. Gaita-Ariño, A.; Prima-García, H.; Cardona-Serra, S.; Escalera-Moreno, L.; Rosaleny, L. E.; Baldoví, J. J. Coherence and organisation in lanthanoid complexes: from single ion magnets to spin qubits. *Inorg. Chem. Front.* **2016**, 3, 568-577, DOI: 10.1039/C5QI00296F.
8. Schleich, W. P. Quantum physics: Engineering decoherence. *Nature* **2000**, 403, 256–257, DOI:10.1038/35002223.
9. Goodwin, C. A. P.; Ortu, F.; Reta, D.; Chilton, N. F.; Mills, D. P. Molecular magnetic hysteresis at 60 kelvin in dysprosocenium. *Nature* **2017**, 548, 439–442, DOI: 10.1038/nature23447.
10. Guo, F.-S.; Day, B. M.; Chen, Y.-C.; Tong, M.-L.; Mansikkamäki, Akseli; Layfield, R. A. A Dysprosium Metallocene Single-Molecule Magnet Functioning at the Axial Limit. *Angew. Chem., Int. Ed*. **2017**, 56, 11445–11449, DOI: 10.1002/anie.201705426.
11. Zadrozny, J. M.; Niklas, J.; Poluektov, O. G.; Freedman, D. E. Millisecond Coherence Time in a Tunable Molecular Electronic Spin Qubit. *ACS Cent. Sci.* **2015**, 1 (9), 488–492, DOI: 10.1021/acscentsci.5b00338.
12. Bader, K.; Dengler, D.; Lenz, S.; Endeward, B.; Jiang, S.-D.; Neugebauer, P.; van Slageren, J. Room temperature quantum coherence in a potential molecular qubit. *Nat. Commun.* **2014**, 5, 5304, DOI: 10.1038/ncomms6304.
13. Donati, F.; Rusponi, S.; Stepanow, S.; Wäckerlin, C.; Singha, A.; Persichetti, L.; Baltic, R.; Diller, K.; Patthey, F.; Fernandes, E.; Dreiser, J.; Šljivančanin, Ž.; Kummer, K.; Nistor, C.; Gambardella, P.; Brune, H. Magnetic remanence in single atoms. *Science* **2016**, 352, 318–321, DOI: 10.1126/science.aad9898.
14. Escalera-Moreno, L.; Baldoví, J.J.; Gaita-Ariño, A.; Coronado, E. Spin states, vibrations and spin relaxation in molecular nanomagnets and spin qubits: a critical perspective. *Chem. Sci*. **2018**, 9, 3265-3275, DOI: 10.1039/C7SC05464E.
15. Clemente-Juan, J. M.; Coronado, E.; Gaita-Ariñoa, A. Magnetic polyoxometalates: from molecular magnetism to molecular spintronics and quantum computing. *Chem. Soc. Rev.* **2012**, 41(22), 7464–7478, DOI: 10.1039/c2cs35205b.
16. Cardona-Serra, S.; Clemente-Juan, J. M.; Coronado, E.; Gaita-Ariño, A.; Camón, A.; Evangelisti, M.; Luis, F.; Martínez-Pérez, M. J.; Sesé, J. Lanthanoid Single-Ion Magnets Based on Polyoxometalates with a 5-fold Symmetry: The Series $[LnP_5W_{30}O_{110}]^{12-}$ (Ln^{3+} = Tb, Dy, Ho, Er, Tm, and Yb). *J. Am. Chem. Soc*. **2012**, 134 (36), 14982–14990, DOI: 10.1021/ja305163t.
17. Shiddiq, M.; Komijani, D.; Duan, Y.; Gaita-Ariño, A.; Coronado, E.; Hill, S. Enhancing coherence in molecular spin qubits via atomic clock transitions. *Nature* **2016**, 531, 348–35, DOI: 10.1038/nature16984.
18. Baldoví, J.J.; Cardona-Serra, S.; Clemente-Juan, J. M.; Coronado, E.; Gaita-Ariñoa, A.; Prima-García, H. Coherent manipulation of spin qubits based on polyoxometalates: the case of the single ion magnet $[GdW_{30}P_5O_{110}]^{14-}$. *Chem. Commun*. **2013**, 49, 8922–8924, DOI: 10.1039/C3CC44838J.
19. Baldoví, J.J.; Duan, Y.; Bustos, C.; Cardona-Serra, S.; Gouzerh, P.; Villanneau, R.; Gontard, G.; Clemente-Juan, J. M.; Gaita-Ariño, A.; Giménez-Saiz, C.; Proust, A.; Coronado, E. Single ion magnets based on lanthanoid polyoxomolybdate complexes. *Dalton Trans*. **2016**, 45, 16653-16660, DOI: 10.1039/C6DT02258H.
20. Baldoví, J.J; Rosaleny, L. E.; Ramachandran, V.; Christian, J.; Dalal, N. S.; Clemente-Juan, J. M.; Yang, P.; U. Kortz, Gaita-Ariño, A.; Coronado, E. Molecular spin qubits based on lanthanide ions encapsulated in cubic

polyoxopalladates: design criteria to enhance quantum coherence. *Inorg. Chem. Front.* **2015**, 2, 893-897, DOI: 10.1039/C5QI00142K.

21. Delferro, M.; Graiff, C.; Elviri, L.; Predieri, G. Self-assembly of polyoxoselenitopalladate nanostars $[Pd_{15}(\mu_3\text{-}SeO_3)_{10}(\mu_3\text{-}O)_{10}Na]^{9-}$ and their supramolecular pairing in the solid state. *Dalton Trans.* **2010**, 39, 4479-4481, DOI: 10.1039/B927537A.
22. Lin, Z.-G.; Wang, B.; Cao, J.; Chen, B.-K.; Gao, Y.-Z.; Chi, Y.-N.; Xu, C..; Huang, X.-Q.; Han, R.-D.; Su, Shuang-Yue; Hu, C.-W. Cation-Induced Synthesis of New Polyoxopalladates. *Inorg. Chem.* **2012**, 51 (8), 4435–4437 DOI: 10.1021/ic300428g.
23. Yang, P.; Xiang, Y.; Lin, Z.; Lang, Z.; Jiménez-Lozano, P.; Carbó, J. J.; Poblet, J. M.; Fan, L.; Hu, C.; Kortz, U. Discrete Silver(I)-Palladium(II)-Oxo Nanoclusters, $\{Ag_4Pd_{13}\}$ and $\{Ag_5Pd_{15}\}$, and the Role of Metal-Metal Bonding Induced by Cation Confinement. *Angew. Chem. Int. Ed.* **2016**, *55*, 15766-15770, DOI: 10.1002/anie.201608122.
24. Xu, F.; Scullion, R. A.; Yan, J.; Miras, H. N.; Busche, C.; Scandurra, A.; Pignataro, B.; Long, D.; Cronin, L. A Supramolecular Heteropolyoxopalladate $\{Pd_{15}\}$ Cluster Host Encapsulating a $\{Pd_2\}$ Dinuclear Guest: $[Pd^{II}_2\subset\{H_7Pd^{II}_{15}O_{10}(PO_4)_{10}\}]^{9-}$. *J. Am. Chem. Soc.* **2011**, *133*, 4684-4686, DOI: 10.1021/ja1105514.
25. Izarova, N. V.; Biboum, R. N.; Keita, B.; Mifsud, M.; Arends, I. W. C. E.; Jameson, G. B.; Kortz, U. Self-assembly of star-shaped heteropoly-15-palladate(II). *Dalton Trans.* **2009**, 9385-9387, DOI: 10.1039/B917079K.
26. (a) te Velde, G.; Bickelhaupt, F. M.; Baerends, E. J.; Guerra, C. F.; Van Gisbergen, S. J. A.; Snijders, J. G.; Ziegler, T. J. *Comput. Chem.* **2001**, 22, 931– 967, DOI: 10.1002/jcc.1056. (b) ADF 2017, SCM, Theoretical Chemistry, Vrije Univesity, Amsterdam, The Netherlands, http://www.scm.com.
27. Izarova, N.; Lin, Z.; Yang, P.; Kondinski, A.; Vankova, N.; Heine, T.; Kortz, U. The polyoxo-22-palladate(II), $[Na_2Pd^{II}_{22}O_{12}(As^{V}O_4)_{15}(As^{V}O_3OH)]^{25-}$. *Dalton Trans.* **2016**, 45, 2394-2398, DOI: 10.1039/C5DT04526F.
28. Kondinski, A.; Vankova, N.; Schinle, F.; Jäger, P.; Hampe, O.; Kortz, U.; Heine, T. How Counterions Affect the Solution Structure of Polyoxoaurates: Insights from UV-Vis Spectral Simulations and Electrospray Mass Spectrometry. *Eur. J. Inorg. Chem.* **2014**, 3771–3778, DOI: 10.1002/ejic.201402494.
29. Izarova, N.; Kondinski, A.; Vankova, N.; Heine, T.; Jäger, P.; Schinle, F.; Hampe, O.; Kortz, U. The mixed gold-palladium polyoxo-noble-metalate, $[NaAu^{III}_4Pd^{II}_8O_8(AsO_4)_8]^{11-}$. *Chem. Eur. J.* **2014**, 20, 8556–8560, DOI: 10.1002/chem.201403032.
30. Barsukova-Stuckart, M.; Izarova, N. V.; Barrett, R.; Wang, Z.; van Tol, J.; Kroto, H. W.; Dalal, N. S.; Keita, B.; Heller, D.; Kortz, U. 3 d Metal Ions in Highly Unusual Eight-Coordination: The Phosphate-Capped Dodecapalladate(II) Nanocube. *Chem. Eur. J.* **2012**, 18, 6167-6171, doi:10.1002/chem.201200060.
31. Shannon, R. D. Revised Effective Ionic Radii and Systematic Studies of Interatomie Distances in Halides and Chaleogenides. *Acta Cryst.*, **1976**, A32, 751-767, DOI: 10.1107/S0567739476001551.
32. Baldoví, J. J.; Borrás-Almenar, J. J.; Clemente-Juan, J. M.; Coronado, E.; Gaita-Ariño, A. Modeling the properties of lanthanoid single-ion magnets using an effective point-charge approach. *Dalton Trans.* **2012**, 41, 13705-13710, DOI: 10.1039/C2DT31411H.
33. Baldoví, J. J.; Cardona-Serra, S.; Clemente-Juan, J. M.; Coronado, E. Gaita-Ariño, A.; Palii, A. SIMPRE: A software package to calculate crystal field parameters, energy levels, and magnetic properties on mononuclear lanthanoid complexes based on charge distributions. *J. Comput. Chem.* **2013**, 34, 1961-1967, DOI: 10.1002/jcc.23341.
34. Baldoví, J.J.; Duan, Y.; Morales, R.; Gaita-Ariño, A.; Ruiz E.; Coronado, E. Rational Design of Lanthanoid Single-Ion Magnets: Predictive Power of the Theoretical Models. *Chem. Eur. J.* **2016**, 22, 13532-13539, DOI: 10.1002/chem.201601741.
35. Baldoví, J. J.; Gaita-Ariño, A.; Coronado, E. Modeling the magnetic properties of lanthanide complexes: relationship of the REC parameters with Pauling electronegativity and coordination number. *Dalton Trans.* **2015**, 44, 12535–12538, DOI: 10.1039/C5DT01839K.
36. Rinehart. J.D.; Long, J.R. Exploiting single-ion anisotropy in the design of f-element single-molecule magnets. *Chem. Sci.* **2011**, 2, 2078-2085, DOI: 10.1039/C1SC00513H.